Title

Mutant p53 regulates enhancer-associated H3K4 monomethylation through interactions with the methyltransferase MLL4

Journal

Journal of Biological Chemistry, 293(34)

ISSN

0021-9258

Authors

Rahnamoun, Homa
Hong, Juyeong
Sun, Zhengxi
et al.

Publication Date

2018-08-01

DOI

10.1074/jbc.ra118.003387

Peer reviewed

JBC Papers in Press. Published on June 28, 2018 as Manuscript RA118.003387
The latest version is at http://www.jbc.org/cgi/doi/10.1074/jbc.RA118.003387

Mutant p53 regulates enhancer-associated H3K4 monomethylation through interactions with the methyltransferase MLL4

Homa Rahnamoun[1], Juyeong Hong[1], Zhengxi Sun[1], Jihoon Lee[1], Hanbin Lu[1], and Shannon M. Lauberth[1*]

From the[1] Section of Molecular Biology, University of California, San Diego, 9500 Gilman Drive, La Jolla, CA 92093, USA

Running Title: Mutant p53 co-opts with MLL4 to regulate enhancer activity.

*To whom correspondence should be addressed: Shannon M. Lauberth: Section of Molecular Biology, University of California San Diego, San Diego, CA 92093-0322; slauberth@ucsd.edu; Tel. (858) 822-0630.

Keywords: histone methylation, inflammation, colon cancer, p53, transcription enhancer, gene regulation

ABSTRACT

Monomethylation of histone H3 lysine 4 (H3K4me1) is enriched at enhancers that are primed for activation and the levels of this histone mark are frequently altered in various human cancers. Yet, how alterations in H3K4me1 are established and the consequences of these epigenetic changes in tumorigenesis are not well understood. Using ChIP-seq in human colon cancer cells, we demonstrate that mutant p53 depletion results in decreased H3K4me1 levels at active enhancers that reveal a striking colocalization of mutant p53 and the H3K4 monomethyltransferase MLL4 following chronic tumor necrosis factor alpha (TNF-α) signaling. We further reveal that mutant p53 forms physiological associations and direct interactions with MLL4 and promotes the enhancer binding of MLL4, which is required for TNF-α-inducible H3K4me1 and histone H3 lysine 27 acetylation (H3K27ac) levels, enhancer-derived transcript (eRNA) synthesis, and mutant p53-dependent target gene activation. Complementary *in vitro* studies with recombinant chromatin and purified proteins demonstrate that binding of the MLL3/4 complex and H3K4me1 deposition is enhanced by mutant p53 and p300-mediated acetylation, which in turn reflects a MLL3/4-dependent enhancement of mutant p53 and p300-dependent transcriptional activation. Collectively, our findings establish a mechanism in which mutant p53 cooperates with MLL4 to regulate aberrant enhancer activity and tumor promoting gene expression in response to chronic immune signaling.

Enhancers regulate gene expression during development and signal-dependent cellular responses(1-6). The location and activity state of enhancers is well correlated with particular epigenetic signatures(6). Specifically, monomethylation of histone H3 lysine 4 (H3K4me1) is enriched at enhancers that are primed for activation, and the accumulation of H3K4me1 and H3 lysine 27 acetylation (H3K27ac) denotes active enhancers(5,7-12). Recent studies have revealed that MLL3 (KMT2C) and MLL4 (KMT2D) constitute the major mammalian histone monomethyltransferases that exhibit partial functional redundancy at enhancers(13,14). MLL3/4 contribute to the regulation of enhancer activation, in part through their recruitment of the histone acetyltransferase (HAT) p300 that mediates H3K27 acetylation(13-16). While the enrichment of MLL3 and MLL4 is well correlated with and predictive of enhancer activity, the factors and mechanisms governing MLL3 and MLL4 recruitment to cell-type and signal-specific enhancers remain poorly understood.

Genome-wide studies have revealed that enhancers are common targets for genetic and epigenetic alterations that are a significant driving force for all types of human cancers(17-23). Specifically, gains and losses in H3K4me1 accumulation at enhancers have been reported in human cancers(17),(24,25) suggesting that alterations in this chromatin modification may lead to enhancer and gene misregulation. In addition, the *MLL3* and *MLL4* genes are frequently mutated, resulting in various developmental defects and cancers(26-28), which may result in the misregulation of H3K4me1 deposition and associated enhancer activation. However, the steps required to establish epigenetic alterations at enhancers that are linked to oncogenic gene expression programs remain poorly understood. Of special interest here is the connection between epigenetic alterations and mutations in the tumor suppressor *p53,* which is the most frequently altered gene found in human cancer(29).

The majority of *p53* mutations are missense and are located in p53's conserved DNA binding domain. The resulting mutant p53 proteins reveal an inactivation of p53 tumor suppressor functions and gain-of-function (GOF) activities that contribute to tumor development(30-32). Increasing evidence has linked GOF properties to the gene regulatory roles of p53 mutants that are largely mediated through mutant p53 recruitment by other transcription factors to promoter and enhancer regions(33-38). In this regard, mutant p53 has recently been shown to cooperate with the master proinflammatory regulator NFκB to regulate enhancer and gene activation in response to chronic tumor necrosis factor alpha (TNF-α) signaling with implications for colon cancer aggressiveness(39). However, the mechanisms by which mutant p53 contributes to enhancer regulation and alterations in the cancer cell transcriptome remain to be elucidated. Given wild-type p53's role in chromatin regulation, p53 mutants may also affect epigenetic changes in chromatin. However, other than the finding that mutant p53 regulates chromatin pathways by modulating the expression of the chromatin modifying enzymes, *MLL1* and *MLL2*(38), the functional evidence that links chromatin regulation and p53 mutations in tumorigenesis remains elusive.

In the present study, we reveal a novel role for mutant p53 in enhancer regulation that is mediated through its ability to alter the enhancer epigenetic landscape. We have employed cell-free assays with recombinant chromatin templates and purified factors along with cancer cell analyses to reveal that mutant p53 contributes to enhancer activation by directing H3K4me1 deposition through MLL4 recruitment. Our results define a molecular mechanism for mutant p53-MLL4 interactions in directing epigenetic signatures that are linked to aberrant enhancer and tumor promoting gene activation.

Results

$p53^{R273H,P309S}$ and MLL4 co-localize at active enhancers and form physiological associations in colon cancer cells

The recent observation that mutant p53 through direct interactions with NFκB is recruited to a class of active enhancers in a manner that parallels with H3K4me1 accumulation in response to chronic TNF-α signaling(39) raised the question whether mutant p53 regulates the enhancer epigenetic landscape. To begin to address this question, we performed chromatin immunoprecipitation followed by sequencing (ChIP-seq) using an antibody specific to MLL4 (KMT2D) in SW480 cells that express p53 with two point mutations, R273H and P309S (hereafter denoted as mutp53) and treated with TNF-α for 16 hr. As demonstrated in Fig. 1A, stringent MLL4 peaks (n=31,082; FDR<0.001) were identified that showed a striking colocalization with mutp53 binding peaks identified in our previously published mutp53 ChIP-seq data that was also performed in SW480 cells treated with TNF-α for 16 hr(39). Approximately 68% of the MLL4 binding sites show overlap with mutp53 and conversely, 58% of the mutp53-occupied regions overlap with MLL4 peaks in response to chronic TNF-α signaling (Fig. 1A). To determine whether mutp53 and MLL4 binding overlap at active enhancers, comparative analyses of our MLL4 ChIP-seq data and our previously published ChIP-seq data(39) for mutp53 and the enhancer-associated histone marks, H3K4me1 and H3K27ac were performed. As shown in the heat maps (Fig. 1B), remarkably, 4,011 active enhancers were identified that are co-occupied by mutp53 and MLL4 in response to chronic TNF-α signaling. We also compared our previously published global run-on sequencing (GRO-seq) data in SW480 cells (39) with the MLL4 and mutp53 ChIP-seq data and found a striking parallel between the mutp53 and MLL4 binding profiles and GRO-seq signals in response to chronic TNF-α signaling (Fig. 1B). This strong parallel between mutp53 and MLL4 binding at active enhancers in response to chronic TNF-α signaling is also demonstrated by the UCSC genome browser tracks of mutp53, MLL4, H3K27ac, and H3K4me1 ChIP-seq data and GRO-seq signals at the *MMP9* and *CCL2* enhancers (Fig. 1C), which are among the signal-dependent enhancers that we recently found are bound and activated by mutp53 and NFκB in response to chronic immune signaling(39).

Given the striking overlap of mutp53 and MLL4 binding profiles, we next assessed whether these factors associate with each other under physiological conditions. As shown in Fig. 1D (left), an anti-p53, but not IgG antibody comparably coimmunopreciptiated mutp53 from SW480 whole cell lysates prepared before and following TNF-α treatment. In addition, mutp53 was found to coimmunoprecipitate ASH2L and RBBP5 subunits that are shared among the members of the SET1/MLL family and the MLL3/4-specific subunit, UTX (Fig. 1D). Notably, the reciprocal coimmunoprecipitation using an anti-MLL4 antibody

also revealed an association of MLL4 with mutp53 and several subunits of the MLL3/4 complex (MLL3/4C) that include UTX, ASH2L, and RBBP5 (Fig. 1D, right). These results demonstrate an association between mutp53 and MLL3/4C that is consistent with the TNF-α-induced global overlap of MLL4, mutp53, H3K4me1, H3K27ac, and the enrichment of enhancer-derived transcripts (eRNAs) across the genome.

$p53^{R273H,P309S}$ regulates enhancer-associated H3K4me1 levels in response to chronic immune signaling

Having identified that mutp53 associates and colocalizes with MLL4 at active enhancers following TNF-α treatment, we next wanted to investigate whether mutp53 regulates H3K4me1 deposition. To address this question, we performed ChIP-seq for mutp53 and H3K4me1 in human SW480 colon cancer cells expressing short hairpin RNAs (shRNAs) against p53 and treated with TNF-α for 16 hr. Relative to a non-targeting shRNA against LacZ (control), an shRNA oligonucleotide directed against p53 mRNA significantly reduced mutp53 protein levels both in uninduced and TNF-α-induced cells (Fig. 2A). The p53 shRNA also significantly decreased MLL2 protein levels, which is consistent with a previous observation that mutp53 regulates the expression levels of the *MLL2* gene in breast cancer cells(38). Notably, no change in the protein levels of MLL4 were observed following mutp53 knockdown (Fig. 2A). In the control cells, composite profiles (Fig. 2B), consistent with the heat maps (Fig. 1B) and browser tracks shown in Fig. 1C, demonstrate an overlap of the peak binding sites for mutp53 with the peak sites of H3K4me1 enrichment at intergenic regions in response to chronic TNF-α signaling. Following mutp53 knockdown, a significant loss of mutp53 binding is observed that strikingly parallels with a moderate reduction in H3K4me1 levels (Fig. 2B). In comparison, mutp53 depletion did not affect global H3K4me1 levels as revealed by immunoblot analysis of histone extracts as shown in Fig. 2A, suggesting that the regulation of H3K4me1 deposition by mutp53 is likely to occur in an enhancer-specific manner.

To further investigate the requirement for mutp53 in regulating H3K4me1 levels at specific mutp53 target enhancers, ChIP experiments followed by quantitative PCR (ChIP-qPCR) were performed in uninduced versus TNF-α-induced conditions in control and mutp53 knockdown SW480 cells. As shown in Fig. 2C, low levels of pre-associated mutp53 binding that correlates with low levels of H3K4me1 accumulation were observed before TNF-α signaling and substantial TNF-α-induced increases in mutp53 binding and H3K4me1 levels were identified at the *MMP9* and *CCL2* enhancers (amplicon A), but not at the control regions (amplicon B). Under TNF-α-induced conditions, p53 knockdown resulted in a comparable decrease in mutp53 binding (80% and 72%) at the *MMP9* and *CCL2* enhancers (amplicon A), respectively as compared to the little to no change at the control regions (amplicon B) (Fig. 2C). Consistent with our ChIP-seq data (Fig. 2B), the decreased levels of TNF-α-induced mutp53 binding resulted in a significant and comparable reduction in the TNF-α-induced levels of H3K4me1 (70% and 72%) at the *MMP9* and *CCL2* enhancers, respectively (Fig. 2C). Under uninduced conditions, we identified little to no effect of mutp53 knockdown on H3K4me1 levels, which is consistent with the significantly lower overall levels of mutp53 and H3K4me1 at the enhancers prior to TNF-α signaling (Fig. 2C).

We next investigated whether mutp53-dependent changes in H3K4me1 levels are due to mutp53 regulation of MLL4 enhancer binding by performing MLL4 ChIP-qPCR analyses in control versus mutp53 knockdown SW480 cells. Notably, mutp53 knockdown resulted in a significant decrease in TNF-α-induced MLL4 binding at the *MMP9* and *CCL2* enhancers by approximately 45% and 57%, respectively but not at the control regions (Fig. 2C), which is consistent with the significant decrease in H3K4me1 levels at these enhancers following the loss of mutp53 enhancer binding. Together, our genome-wide binding data parallel our enhancer-specific analyses, demonstrating that mutp53 directly regulates H3K4me1 levels at specific enhancers in response to chronic TNF-α signaling.

p53 R273H directly interacts and facilitates primary MLL3/4C recruitment and cooperates with p300 to enhance MLL3/4 binding on reconstituted chromatin

Having identified functional associations between mutp53 and MLL4 at active enhancers in response to chronic TNF-α signaling in colon cancer cells, we next wanted to investigate the functional relationship between these two factors using biochemical assays. First, to determine whether an intact MLL3/4C forms direct interactions with mutant p53, MLL3/4C was purified to near homogeneity through FLAG-tagged PA1, a unique

subunit of MLL3/4C (Supplementary Figs 1A-C) using established methods(40). *In vitro* binding assays revealed that MLL3/4C bound strongly to GST-p53 R273H, but not to GST alone (Fig. 3A). This finding demonstrates a direct p53 R273H-MLL3/4C interaction that is consistent with the physiological association and the functional interplay between these factors at specific enhancers. We further demonstrated the ability of MLL3/4C to interact with GST-tagged p53 wild-type and the hotspot p53 mutants, R248W and G245S (Supplementary Fig. 1D). The finding that MLL3/4C interacts with wild-type p53 is consistent with the findings of a previous study(41).

We next performed *in vitro* chromatin immunoprecipitation (ChIP) assays as outlined in Fig. 3B to investigate the effects of p53 R273H on MLL4 binding to recombinant chromatin templates. Chromatin was assembled following established protocols(42) and using recombinant factors (Supplementary Fig. 1E), reconstituted histone octamers (Supplementary Fig. 2), and a DNA template that consists of five GAL4 binding sites upstream of the adenovirus (Ad) major late (ML) core promoter and a 390-nucleotide G-less cassette (Fig. 3C). Micrococcal nuclease (MNase) digestion of our chromatinized templates confirmed equivalent nucleosome spacing (Supplementary Fig. 1F). As depicted in Fig. 3B, chromatin was incubated in the presence or absence of recombinant GAL4-p53 R273H, the histone acetyltransferase p300, and MLL3/4C; digested with MNase; and immunoprecipitated with antibodies against p53 R273H or ASH2L, a core subunit of MLL3/4C that is indispensable for its methyltransferase activity(43). The precipitated DNA was analyzed by qPCR using primer sets that scan both the promoter region (amplicon A), containing the GAL4 binding sites, and a distal vector control region (amplicon B) (Fig. 3C). As expected, low levels of p53 R273H binding were identified specifically at the promoter and not the distal control region, which is indicative of the importance of the GAL4 binding sites, which are recognized and bound by GAL4-p53 R273H (Fig. 3D, column 3). As shown in Fig. 3D (column 4 versus 3), p53 R273H binding to recombinant chromatin was largely unaffected by the presence of MLL3/4C. However, ectopic p300 resulted in a substantial (5-fold) increase in p53 R273H binding at the promoter region (Fig. 3D, column 5 versus column 3). Notably, p53 R273H is required to direct MLL3/4C recruitment on chromatin as revealed by the 2-fold increase in ASH2L binding at the promoter (Fig. 3D, column 4 versus column 2), which is consistent with our cell-based ChIP data that revealed a requirement for mutp53 in regulating MLL3/4 enhancer interactions (Fig. 2C). In addition, the enhanced binding of ASH2L mediated by p53 R273H was moderately augmented (~1.3-fold) by ectopic p300 (Fig. 3D, column 7 versus 4). The lack of an effect of p300 alone on ASH2L binding (Fig. 3D, column 6 versus 2) also indicates that the increase in p53 R273H-dependent binding of ASHL2 is likely due to the enhanced p300-mediated stabilization of mutp53 on chromatin (Fig. 3D, column 5 versus 3). Taken together our cell-based and *in vitro* binding data demonstrate that mutp53-MLL3/4C interactions are important for MLL3/4 recruitment on chromatin and that p53 R273H can act cooperatively with p300 to direct enhanced MLL3/4 binding.

MLL3/4C facilitates p53 R273H-dependent H3K4 monomethylation and enhanced transcription

To further investigate the direct (causal) effects of mutant p53-MLL3/4C interactions on chromatin, we next sought to determine whether p53 R273H impacts MLL3/4C-mediated H3K4me1 deposition by employing histone methyltransferase (HMT) assays as denoted in Fig. 4A. An initial analysis on recombinant histone octamers revealed significant and specific effects of the purified MLL3/4C on H3K4 monomethylation and little to no change in di- and trimethylation (Supplementary Fig. 2A). On chromatin templates, p53 R273H-dependent increases in H3K4me1 levels were observed that are significantly (4-fold) above the low/negligible levels of H3K4me1 that are observed by MLL3/4C alone (Fig. 4B, lane 3 versus 2). These findings are consistent with the *in vitro* ChIP data that revealed significant and specific levels of MLL3/4 binding on chromatin templates only in the presence of p53 R273H (Fig. 3D). In addition, the p53 R273H and MLL3/4C-dependent H3K4me1 levels were further enhanced (~6-fold) in the presence of p300, thereby yielding a ~30-fold increase in total H3K4me1 levels (Fig. 4B, lane 5 versus 3). Consistent with our HMT assays in which p300 is able to enhance p53 R273H and MLL3/4-mediated H3K4me1, MLL3/4C, albeit less significantly (1.7-fold), enhanced p53 R273H and p300-dependent acetylation (Supplementary Fig. 2B, lane 5 versus 4). The cooperativity between cofactors, p300 and MLL3/4 on chromatin is consistent with the recently reported identification that MLL4 directly interacts with p300, through the UTX subunit of MLL3/4C and that these interactions result in the cooperative regulation of H3K4me1 and H3K27ac(44).

To determine whether mutp53, MLL3/4C, and p300-dependent deposition of H3K4me1 and H3K27ac directly contribute to mutp53-dependent transcription, we employed a chromatin-templated cell-free transcription system(42) (Figs 4A, C). A significant level of p53 R273H-dependent transcription was observed that is dependent on the presence of p300/acetyl-CoA (Fig. 4C, lane 6 versus lane 2). In comparison to p300, MLL3/4C alone did not support a detectable level of p53 R273H-dependent transcription (Fig. 4C, lane 7 versus 6). Importantly, however, MLL3/4C enhanced (~2-fold) the p53 R273H-dependent transcription signal in the presence of p300/acetyl-CoA (Fig. 4C, lane 12 versus 6), which is consistent with the significantly higher overall levels of H3K4me1 (Fig. 4B) and H3K27ac (Supplementary Fig. 2B) that are observed in the presence of MLL3/4 and p300. In contrast, MLL3/4 in the absence of S-adenosyl methionine (SAM) was unable to enhance p53 R273H/p300-dependent transcriptional activation (Fig. 4C, lane 12 versus 11), which suggests the importance of H3K4me1 in regulating the transcriptional output. Thus, our cell-based findings are corroborated by our *in vitro* mechanistic studies that demonstrate mutant p53 coordinates H3K4me1 through the chromatin targeting of MLL3/4C, which in turn directs enhanced transcriptional activation.

MLL3/4 regulate the activation of p53^{R273H,P309S} bound enhancers in response to chronic TNF signaling

Having established a functional interplay between p53 R273H and MLL3/4C in regulating H3K4me1 deposition and transcriptional activation on recombinant chromatin, we next examined a direct role for MLL3/4C in the regulation of mutp53 enhancers and target genes in response to chronic immune signaling. Given the previously reported functional redundancy of MLL3 and MLL4(13,14), we generated MLL3/4 double knockdown SW480 cells in which the protein levels of both MLL3 and MLL4 were significantly reduced (Supplementary Fig. 3A). Under uninduced conditions, MLL3/4 knockdown resulted in little to no effect on MLL4 binding, H3Kme1, or H3K27ac levels at the enhancer regions of *MMP9* and *CCL2,* which is further indicative of the specific binding and roles of MLL4 at mutp53-dependent enhancers in response to chronic TNF-α signaling (Fig. 5A). In TNF-α treated cells, MLL3/4 knockdown caused substantial losses (53% and 47%) in the TNF-α induced binding of MLL4 at the enhancer regions of *MMP9* and *CCL2*, respectively as compared to nonspecific control regions (Fig. 5A). In addition, this loss of MLL4 enhancer binding is accompanied by a notable (~50%) reduction in H3K4me1 levels at both the *MMP9* and *CCL2* enhancers (Fig. 5A). While the enhancer-specific H3K4me1 levels were significantly affected by the loss of MLL4 binding, the global H3K4me1 levels remained largely unaffected as revealed by immunoblot analyses of histone extracts prepared from identical cell lines (Supplementary Fig. 3A). Also, consistent with a role for MLL3/4 in the activation of the *MMP9* and *CCL2* enhancers, we identified that the TNF-α-induced accumulation of H3K27ac at these enhancers was also significantly reduced (63% and 56%, respectively) following MLL3/4 depletion (Fig. 5A). Moreover, qRT-PCR analyses revealed a ~2-fold reduction in the TNF-α induced expression levels of both the *MMP9* and *CCL2* eRNAs following MLL3/4 knockdown (Fig. 5B), which also correlated with a decrease in the TNF-α induced mRNA expression levels of *MMP9* and *CCL2* (1.8-fold and 11-fold, respectively). Consistent with these changes in enhancer transcription and gene expression, we also identified that MLL3/4 depletion results in a notable (~55%) reduction in the TNF-α induced binding of RNAPII at the enhancer versus nonspecific control regions of *MMP9* and *CCL2* (Supplementary Fig. 3B). This loss of TNF-α induced RNAPII binding is not due to MLL3/4-dependent stabilization of mutp53 binding since MLL3/4 depletion did not affect the TNF-α induced binding of mutp53 at these enhancers (Supplementary Fig. 3B). Moreover, the lack of an effect on mutp53 binding in MLL3/4 depleted cells is consistent with our *in vitro* ChIP data that show p53 R273H binding is largely unaffected by the presence of MLL3/4C, whereas p53 R273H is required to regulate MLL3/4C recruitment on reconstituted chromatin.

Having previously established TNF-α and mutp53-dependent alterations in the colon cancer cell transcriptome that are associated with an increase in invasive potential(39), we next wanted to explore whether MLL4-dependent epigenetic alterations that are linked to changes in mutp53-dependent gene expression contribute to an increase in cancer cell invasion. As revealed in Fig. 5C, cell invasion assays revealed that TNF-α treatment results in a ~10-fold increase in the number of control cells that pass through the Matrigel. Notably however, MLL3/4 depletion markedly reduced the number of invading cells following TNF-α signaling by ~7-fold (Fig. 5C).

Collectively, these findings establish a requirement for MLL4 in regulating TNF-α-induced alterations in enhancer and tumor promoting gene activation that are linked to enhanced cancer cell invasion.

Discussion

In this study, we demonstrated that mutant p53 modulates the chromatin landscape through interactions with MLL3/4. An association between mutant p53 and MLL3/4 was maintained during high stringency immunoprecipitation experiments and binding assays with recombinant purified proteins. Consistent with the identified mutp53-MLL3/4 interactions, our current study also provides insight into a mechanism in which mutp53 regulates the recruitment of MLL3/4 to chromatin. Specifically, we show that p53 R273H is required for the direct and primary recruitment of MLL3/4C to reconstituted chromatin templates in our cell-free assays. We also establish a requirement for mutp53 in regulating MLL4 recruitment at specific enhancers in response to chronic immune signaling as demonstrated by the significant loss of MLL4 binding following mutp53 depletion. Overall, our results provide strong evidence for a functional relationship between mutp53 and MLL3/4 at specific enhancers following chronic immune signaling. Given that a relatively high number of amino acid residues in the p53 C-terminal domain (CTD) are modified by several posttranslational marks including methylation(45,46), future analysis will address the significance of mutp53-MLL3/4 associations in relation to mutp53 regulation via methylation and/or demethylation mediated by the various subunits of MLL3/4. Such analyses will provide additional insights into mechanisms underlying mutp53-dependent enhancer and gene regulation to advance our understanding of mutp53 GOF properties in human cancer.

Our study highlights an emerging link between wild-type MLL4 and mutp53 in defective enhancer regulation and the activation of tumor promoting gene expression. Support for the mechanistic crosstalk between mutp53 and MLL4 at specific enhancers is demonstrated by MLL4 depletion that leads to a loss in the deposition of H3K4me1 and H3K27ac. Under these conditions, concomitant downregulation of RNAPII binding, eRNA synthesis, and mutp53-dependent gene activation was also observed. In addition, we demonstrate that the enhancer-directed alterations in mutp53 target gene activation mediated by MLL4 and TNF-α are associated with the biological consequence of increased cancer cell invasion.

While our study provides insight into an underlying mechanism for the functional relationship between wild-type MLL4 and mutp53, future analyses will be directed at unraveling the significance of an association between mutp53 and mutant forms of MLL4. This is supported by previous studies that have demonstrated that *MLL4* is among the most recurrently mutated epigenetic enzymes in human cancers including glioblastoma, melanoma, pancreatic, and breast cancers(27,28,47). Characterization of a potential convergence between mutp53 and mutant MLL4 will further advance our understanding of the multi-dimensional regulation of gene networks in human cancer. It is also noteworthy that we identified a mutp53-dependent regulation of MLL2 as revealed by the significant decrease in MLL2 protein levels in colon cancer cells following mutp53 depletion. This finding is consistent with a previous report showing that mutp53 controls chromatin pathways by regulating the expression of the SET/MLL family members, *MLL1* and *MLL2* in breast cancer(38). These findings together with our study which shows that mutp53 does not regulate MLL4 protein levels but instead forms functional interactions with MLL4 to regulate enhancer activation, indicate the importance of differential histone methylation mechanisms modulated by mutp53 and the various SET/MLL family members.

A direct mechanistic link between MLL3/4C-mediated methylation, p300-mediated acetylation, and augmented p53 R273H-dependent transcriptional activation was revealed by employing purified proteins, reconstituted chromatin templates, and cell-free assays. We found that while MLL3/4-mediated H3K4me1 does not play a primary function in regulating p53 R273H-dependent transcription, this epigenetic change contributes to enhanced transcriptional output in a p53 R273H/p300-dependent manner. A recent report demonstrated direct interactions between MLL3/4 (UTX subunit) and p300 that promote enhancer activation and in turn, boost transcriptional activation by all-trans retinoic acid ATR(44). The reciprocal functional interplay between MLL3/4-mediated H3K4me1 and p300-mediated acetylation that is required for enhanced transcriptional activation by mutp53 and ATR could provide an explanation for the recent reports that demonstrate a significantly reduced effect of catalytically inactive SET domain mutants of MLL3/4 versus MLL3/4 depletion on enhancer transcription(48). It is also noteworthy that the stimulatory effect on p53 R273H/p300-dependent transcription that is specifically observed for

MLL3/4-dependent H3K4me1 versus MLL3/4 in the absence of H3K4me1 (devoid of SAM) provides evidence to support a role of the histone mark H3K4me1 itself in regulating transcriptional activation. A potential role for H3K4me1 in enhancer activation could be mediated through specific H3K4me1 reader proteins that are present in the nuclear extract that is used in our cell-free system. One possible factor could be TIP60, a HAT protein that preferentially binds to H3K4me1 through its chromodomain(49). Further support for this proposed mechanism is also provided by the recent finding that H3K4me1 through the recruitment of Cohesin complexes is required to support chromatin interactions at enhancers(50). In this study, we advance previous analyses of enhancer malfunction in human cancer by revealing a new role for a GOF mutant of the tumor suppressor *p53* in shaping the chromatin landscape. Mutp53 and NFκB were previously shown to contribute to each other's recruitment at a subset of cancer cell-specific enhancers that are linked to the activation of a tumor promoting gene expression program in response to chronic immune signaling(51). While we demonstrate that p53 wild-type can also interact with the MLL3/4C, which is consistent with the previously reported cofactor role of MLL3/4C in the regulation of wild-type p53 tumor suppressor functions(41), it is important to note that the subset of enhancers that were analyzed in this study were previously found to be exclusively bound by mutant and not wild-type p53(39). As depicted in the proposed model (Fig. 6), our study demonstrates the significance of mutp53 through interactions with MLL4 in regulating the activation of these mutp53 bound enhancers. The identification of this epigenetic mechanism underlying alterations in enhancer-specific histone modifications, enhancer transcription, and the potent induction of mutp53 target genes establishes a new functional link between mutp53 and chromatin pathways in colon cancer cells that are stimulated by chronic TNF-α signaling.

EXPERIMENTAL PROCEDURES

Cell culture

Human colorectal adenocarcinoma SW480 cells and human embryonic kidney 293T (HEK293T) cells were purchased from American Type Culture Collection (ATCC) and grown in Dulbecco's modified Eagle medium (DMEM, Gibco), supplemented with 10% fetal bovine serum (FBS, Gibco). Lentivirus infected SW480 cells were propagated in DMEM containing 10% FBS and 1.5 μg ml^{-1} puromycin (Sigma). Stable and inducible SW480 control and p53 knockdown cells that express short hairpins against LacZ or p53 were kindly provided by Xinbin Chen (UC Davis) and were grown in standard DMEM medium containing 1X penicillin/streptomycin (Gemini Bio-Products) and 1.5 μg ml^{-1} puromycin, and were induced with 1 μg ml^{-1} doxycycline (Sigma). For experiments with TNF-α treatment, the indicated cells were treated with 12.5 ng ml^{-1} recombinant human TNF-α (Shenandoah Biotechnology) for 0 or 16 hr before harvesting for gene expression or ChIP analyses.

Lentivirus production and transduction

PLKO.1 TRC control and target shRNAs were generated with annealed primers to knockdown MLL3 and MLL4. For lentivirus production, HEK293T cells were transfected using Lipofectamine 2000 (Invitrogen) with control or target shRNAs and packaging plasmids psPAX2 and pMD2.G. Medium containing the virus was collected 48 hr post transfection and used for infection. SW480 cells were infected with virus containing medium in the presence of 8 μg ml^{-1} polybrene (Sigma) for 8 hr and subsequently selected with 1.5 μg ml^{-1} puromycin. Target shRNA sequences are listed in Supplementary Table 1.

RNA purification and quantitative real-time PCR

Total RNA was isolated from cells using TRIzol LS reagent (Invitrogen) according to the manufacturer's instructions. cDNA synthesis was performed using ProtoScript II First Strand cDNA Synthesis Kit (NEB) with random hexamers. qPCR reactions were performed on an Applied Biosystems Step One Plus real-time PCR systems using SYBR Green PCR Master Mix (Applied Biosystems) in duplicates and the amplification specificity was examined by melting curve analysis. The relative levels of eRNA and mRNA expression were calculated according to the (ΔΔCt) method and normalized to *GAPDH*. The expression levels determined after TNF-α treatment are relative to the levels before TNF-α treatment. Primers for qRT-PCR are listed in Supplementary Table 2.

Invasion assay

SW480 cells stably expressing control or MLL3/4 shRNAs were pre-treated with or without 12.5 ng ml^{-1} TNF-α in low serum media (0.1%) for 24 hr prior to plating 2-4 $x10^5$ cells from each condition on 24-well PET inserts with 8.0mm pore size (Falcon), coated with BD Matrigel (BD Bioscience). The lower chambers were filled with high serum

media (20%) without TNF-α. Cells that passed through the Matrigel after 24hr were fixed, stained, and counted. Representative scale bars were added using ImageJ.

Immunoblotting
Protein samples were incubated at 95 °C for 5 min, resolved by SDS-PAGE, and transferred to PVDF membranes (EMD Millipore) that were subsequently blocked and probed with the indicated antibodies. For MLL3/4 detection, protein samples were resolved on a 3-8% tris acetate gel (Life Technologies). Reactive bands were detected by ECL (Thermo Scientific Pierce), and exposed to Blue Devil Lite ECL films (Genesee Scientific) for visualization.

Antibodies
The following antibodies were used for ChIP and immunoblotting analyses: anti-H3 (Abcam, ab1791), anti-H3K4me1 (Abcam, ab8895) and anti-H3K4me2 (Abcam, ab11946), anti-H3K4me3 (Abcam, ab8580), p53 (Santa Cruz Biotechnology, sc-126), anti-IgG (Santa Cruz Biotechnology, sc-2027), anti-β-Actin (Santa Cruz Biotechnology, sc-47778), anti-RBBP5 (Bethyl Laboratories, A300-109A), anti-ASH2L (Bethyl Laboratories, A300-489A). Anti-PTIP and anti-UTX antibodies were kindly provided by Robert Roeder (Rockefeller University, New York, NY) while anti-MLL3 and anti-MLL4 antibodies were provided by Kai Ge (National Institutes of Health, Bethesda, MD).

Co-Immunoprecipitation
Whole cell lysates were prepared from SW480 cells that were treated with 12.5 ng ml^{-1} TNF-α for 0 or 16 hr and lysed with the following buffer (20 mM Tris-HCl pH7.5, 150 mM NaCl, 0.5% NP-40, 0.5% Triton X-100, 2 mM EDTA), supplemented with protease inhibitor cocktail (PIC) (Sigma) on ice for 30 mins. Cleared lysates were incubated with the indicated antibodies overnight at 4 ºC, followed by incubation with protein A Dynabeads (Life Technologies) for 2 hr at 4 ºC. Beads were subsequently washed with lysis buffer three times prior to elution and analysis of protein complexes by immunoblotting.

MLL3/4 complex purification
HeLaS cells stably expressing FLAG-tagged PA1 were kindly provided by Kai Ge (NIH), grown in DMEM containing 10% FBS and 0.1 mg ml^{-1} G418, and used to isolate a FLAG-PA1-associated MLL3/4 complex as previously described(40). Briefly, 100 mg of nuclear extract was precleared twice with 0.2 ml of mouse IgG-agarose for 2 hr in buffer A (20 mM HEPES at pH 7.9, 180 mM KCl, 0.2 mM EGTA, 1.5 mM $MgCl_2$, 20% glycerol, 0.1% NP-40), followed by overnight immunoprecipitation with 0.2 ml anti-FLAG M2-agarose (Sigma) at 4 ºC. Following several washes with buffer A, bound proteins were eluted twice with 0.25 mg ml^{-1} FLAG peptide (Sigma) and concentrated with Amicon concentrator columns (Millipore).

Recombinant protein purification and *in vitro* binding assays
Glutathione S-transferase (GST)-tagged p53 WT, R175H, R273H, R248W, and G245S were expressed in *E. coli* Rosetta cells and purified using Glutathione Sepharose 4B (GE Life Sciences). For *in vitro* binding assays, the MLL3/4 complex was precleared with Glutathione Sepharose beads for 30 min at 4 ºC, and then incubated with 1.5 ug of the GST fusion proteins overnight at 4 ºC in binding buffer (25 mM HEPES-KOH at pH 7.8, 150 mM NaCl, 0.1% NP-40, 1.5 mM $MgCl_2$, 10% glycerol). The bound proteins were washed three times with binding buffer, eluted, and analyzed by immunoblotting.

Chromatin Immunoprecipitation (ChIP) and ChIP-Seq
SW480 cells were treated with i) 12.5 ng ml^{-1} TNF-α for 0 or 16 hr or ii) indicated shRNAs and subsequently exposed to 12.5 ng ml^{-1} TNF-α for 0 or 16 hr. Cells were crosslinked in 6 mM disuccinimidyl glutarate (DSG) (ProteoChem) in PBS for 30 min at room temperature followed by the addition of 1% final formaldehyde concentration for 10 min at room temperature. Crosslinking was quenched with 0.125 mM glycine (Fisher Scientific). Cell pellets were resuspended in lysis buffer (20 mM Tris-HCl at pH 7.5, 300 mM NaCl, 2 mM EDTA, 0.5% NP-40, 1% Triton X-100, 1 mM PMSF, PIC) and incubated on ice for 30 min, followed by homogenization. Nuclear pellets were collected and resuspended in shearing buffer (0.1% SDS, 0.5% N-lauroylsarcosine, 1% Triton X-100, 10 mM Tris-HCl at pH 8.1, 100 mM NaCl, 1 mM EDTA, 1 mM PMSF, PIC) and chromatin was fragmented to an average size of 200-500 bp with a bioruptor Pico (Diagenode). Precleared chromatin was immunoprecipitated with the indicated antibodies overnight at 4 ºC and immunocomplexes were collected with protein A Dynabeads. The immunocomplexes were washed eight times in wash buffer (50 mM HEPES-KOH at pH 7.6, 500

mM LiCl, 1 mM EDTA, 1% NP-40, 0.7% sodium deoxycholate, 1 mM PMSF, PIC), followed by two TE washes, and subsequently eluted in elution buffer (50 mM Tris-HCl at pH 8.0, 10 mM EDTA, 1% SDS). The eluates were incubated overnight at 65 ºC to reverse the crosslinks and ChIP DNA was purified using DNA Clean & Concentrator Kit (Zymo Research) according to the manufacturer's instructions before qPCR analysis on an Applied Biosystems Step One Plus real-time PCR systems using SYBR Green PCR Master Mix in duplicates. The relative amounts of ChIP DNA were quantified relative to corresponding input samples. Primers for ChIP-qPCR are listed in Supplementary Table 3. For ChIP-seq experiments, the IPs were performed as described above. The eluted ChIP DNA was quantitated using a Qubit 2.0 fluorometer (Invitrogen), and 1-5 ng of ChIP DNA was used to prepare the sequencing libraries from at least two biological replicates using the ChIP TruSeq Sample Prep Kit according to the manufacturer's instructions (Illumina). Briefly, ChIP DNA samples were end-repaired and adaptors were ligated to the ends of the DNA fragments. Adaptor-ligated ChIP DNA fragments with average size of 350 bp were used to construct libraries and single-end sequenced (75 bp) on Illumina HiSeq 4000. Reads were mapped to hg38 human genome using Bowtie2 software 38 and default parameters. The mapped reads were then processed to make Tag Directory module using HOMER for filtering. Briefly, PCR duplications were removed and only uniquely mapped reads were kept for further analysis. Enrichment for $p53^{R273H,P309S}$ and H3K4me1 deposition were called using findPeaks module from HOMER using preset parameters for transcription factors and histones, respectively and compared to the input samples. The genome browser files for the resulting reads were generated by using makeUCSCfile module from HOMER. Deeptools were used to generate heat maps.

Recombinant Chromatin Assembly, *in vitro* ChIP, HAT, and HMT Assays

In vitro chromatin assembly was performed as previously described(42) using a pG_5ML DNA template containing 5x GAL4 response elements and reconstituted histone H3 octamers, ACF1, ISWI, and NAP1. HAT assays contained 150 ng of chromatin, 100 ng of GAL4-p53 R273H, 30 ng of p300, and 20 μM acetyl CoA, 1 μl of concentrated MLL3/4C, and 20 μM SAM in reaction buffer (50 mM HEPES at pH7.8, 30 mM KCl, 0.25 mM EDTA, 5.0 mM $MgCl_2$, 5.0 mM sodium butyrate, 2.5 mM DTT). Reactions were incubated at 30 ºC for 30 min. ChIP, HAT, and HMT assays were performed in two consecutive steps: i) 150 ng of chromatin, 100 ng of GAL4-p53 R273H, 30 ng of p300, and 20 μM acetyl CoA were incubated at 30 ºC for 30 min, followed by ii) addition of 1 μl of the MLL3/4C and 20 μM SAM for an additional incubation at 30 ºC for 60 min. For ChIP assays, reactions were terminated on ice followed by MNase (Sigma) digestion in buffer R (10 mM HEPES at pH 7.9, 10 mM KCl, 0.5 mM EGTA, 10% glycerol) at room temperature for 10 mins. Digestion reactions were then quenched with the addition of 20 mM EDTA and subsequently immunoprecipitated with the indicated antibodies overnight at 4 ºC. Immunocomplexes were washed, eluted, and processed for analysis by qPCR as described above. For HAT and HMT assays, reactions were resolved on 15% SDS-PAGE gels and analyzed by immunoblotting.

***In vitro* Chromatin-Templated Transcription Assays**

Chromatin-templated transcription was performed as described(42) with minor modifications. Transcription steps are as follows: (1) activator binding: GAL4-p53 R273H (100 ng) was incubated with recombinant chromatin template (40 ng) in reaction buffer at 30 ºC for 20 min; (2) chromatin-based histone acetylation: p300 (25 ng) and acetyl CoA (20 μM) were added to the reactions and incubated at 30ºC for 30 min; (3) chromatin-based histone methylation: MLL3/4C and SAM (20 μM) were added to the reactions and incubated at 30ºC for 60 min; (4) transcription: 5.0 μl (10 mg ml^{-1}) of HeLa nuclear extract and nucleotide mixture with 10 μCi of [α-32P] CTP (3000 Ci/mmol; PerkinElmer) were sequentially added to the reaction for 20 min and 50 min at 30 ºC, respectively. The radiolabeled RNA was purified and resolved on 5% polyacrylamide (37.5:1) with 8.0 M urea and analyzed by autoradiography.

Data Availability

All sequencing data that support the findings of this study have been deposited in the National Center for Biotechnology Information Gene Expression Omnibus (GEO) and are accessible through the GEO Series Accession numbers GSE102796 and GSE115985. All other relevant data are available from the corresponding author upon reasonable request.

Acknowledgements
We are grateful to Kai Ge (NIH) for providing the HeLaS cells that stably express FLAG-PA1 as well as MLL3 and MLL4 antibodies, Robert Roeder (Rockefeller University) for providing the UTX and PTIP antibodies, and Xinbin Chen (UC Davis) for providing the SW480 shLacZ and shp53 cell lines. We are also thankful to Danielle Freeman for technical support. This work was supported by the Research Scholar Award from the Sidney Kimmel Foundation for Cancer Research #857A6A and University of California Cancer Research Coordinating Committee, CRN-17-420616 to S.M.L. and the UCSD Cellular and Molecular Genetics Training Program through an institutional grant from the National Institute of General Medicine (T32 GM007240) to H.R.

Author contributions
Conceptualization, H.R. and S.M.L.; Methodology, H.R., J.H., Z.S., J.L., H.L., and S.M.L.; Investigation, H.R., J.H., Z.S., H.L., J.L., and S.M.L.; Formal Analysis, H.R., J.H., H.L., and S.M.L.; Writing - Original Draft, H.R. and S.M.L.; Writing - Review & Editing, H.R., and S.M.L.; Funding Acquisition, S.M.L. and H.R.; Supervision, S.M.L.

Conflict of interest
The authors declare that they have no conflicts of interest with the contents of this article.

References

1. Levine, M. (2010) Transcriptional enhancers in animal development and evolution. *Curr Biol* **20**, R754-763
2. Ong, C. T., and Corces, V. G. (2011) Enhancer function: new insights into the regulation of tissue-specific gene expression. *Nature reviews. Genetics* **12**, 283-293
3. Makova, K. D., and Hardison, R. C. (2015) The effects of chromatin organization on variation in mutation rates in the genome. *Nature reviews. Genetics* **16**, 213-223
4. Levine, M., Cattoglio, C., and Tjian, R. (2014) Looping back to leap forward: transcription enters a new era. *Cell* **157**, 13-25
5. Calo, E., and Wysocka, J. (2013) Modification of enhancer chromatin: what, how, and why? *Mol Cell* **49**, 825-837
6. Heinz, S., Romanoski, C. E., Benner, C., and Glass, C. K. (2015) The selection and function of cell type-specific enhancers. *Nat Rev Mol Cell Biol* **16**, 144-154
7. Chepelev, I., Wei, G., Wangsa, D., Tang, Q., and Zhao, K. (2012) Characterization of genome-wide enhancer-promoter interactions reveals co-expression of interacting genes and modes of higher order chromatin organization. *Cell Res* **22**, 490-503
8. Heintzman, N. D., Hon, G. C., Hawkins, R. D., Kheradpour, P., Stark, A., Harp, L. F., Ye, Z., Lee, L. K., Stuart, R. K., Ching, C. W., Ching, K. A., Antosiewicz-Bourget, J. E., Liu, H., Zhang, X., Green, R. D., Lobanenkov, V. V., Stewart, R., Thomson, J. A., Crawford, G. E., Kellis, M., and Ren, B. (2009) Histone modifications at human enhancers reflect global cell-type-specific gene expression. *Nature* **459**, 108-112
9. Creyghton, M. P., Cheng, A. W., Welstead, G. G., Kooistra, T., Carey, B. W., Steine, E. J., Hanna, J., Lodato, M. A., Frampton, G. M., Sharp, P. A., Boyer, L. A., Young, R. A., and Jaenisch, R. (2010) Histone H3K27ac separates active from poised enhancers and predicts developmental state. *Proc Natl Acad Sci U S A* **107**, 21931-21936
10. Rada-Iglesias, A., Bajpai, R., Swigut, T., Brugmann, S. A., Flynn, R. A., and Wysocka, J. (2011) A unique chromatin signature uncovers early developmental enhancers in humans. *Nature* **470**, 279-283
11. Wang, D., Garcia-Bassets, I., Benner, C., Li, W., Su, X., Zhou, Y., Qiu, J., Liu, W., Kaikkonen, M. U., Ohgi, K. A., Glass, C. K., Rosenfeld, M. G., and Fu, X. D. (2011) Reprogramming transcription by distinct classes of enhancers functionally defined by eRNA. *Nature* **474**, 390-394
12. Rivera, C. M., and Ren, B. (2013) Mapping human epigenomes. *Cell* **155**, 39-55
13. Hu, D., Gao, X., Morgan, M. A., Herz, H. M., Smith, E. R., and Shilatifard, A. (2013) The MLL3/MLL4 branches of the COMPASS family function as major histone H3K4 monomethylases at enhancers. *Mol Cell Biol* **33**, 4745-4754
14. Lee, J. E., Wang, C., Xu, S., Cho, Y. W., Wang, L., Feng, X., Baldridge, A., Sartorelli, V., Zhuang, L., Peng, W., and Ge, K. (2013) H3K4 mono- and di-methyltransferase MLL4 is required for enhancer activation during cell differentiation. *eLife* **2**, e01503
15. Herz, H. M., Mohan, M., Garruss, A. S., Liang, K., Takahashi, Y. H., Mickey, K., Voets, O., Verrijzer, C. P., and Shilatifard, A. (2012) Enhancer-associated H3K4 monomethylation by Trithorax-related, the Drosophila homolog of mammalian Mll3/Mll4. *Genes Dev* **26**, 2604-2620

16. Wang, C., Lee, J. E., Lai, B., Macfarlan, T. S., Xu, S., Zhuang, L., Liu, C., Peng, W., and Ge, K. (2016) Enhancer priming by H3K4 methyltransferase MLL4 controls cell fate transition. *Proc Natl Acad Sci U S A* **113**, 11871-11876
17. Akhtar-Zaidi, B., Cowper-Sal-lari, R., Corradin, O., Saiakhova, A., Bartels, C. F., Balasubramanian, D., Myeroff, L., Lutterbaugh, J., Jarrar, A., Kalady, M. F., Willis, J., Moore, J. H., Tesar, P. J., Laframboise, T., Markowitz, S., Lupien, M., and Scacheri, P. C. (2012) Epigenomic enhancer profiling defines a signature of colon cancer. *Science* **336**, 736-739
18. Aran, D., and Hellman, A. (2013) DNA methylation of transcriptional enhancers and cancer predisposition. *Cell* **154**, 11-13
19. Aran, D., Sabato, S., and Hellman, A. (2013) DNA methylation of distal regulatory sites characterizes dysregulation of cancer genes. *Genome biology* **14**, R21
20. Jia, L., Landan, G., Pomerantz, M., Jaschek, R., Herman, P., Reich, D., Yan, C., Khalid, O., Kantoff, P., Oh, W., Manak, J. R., Berman, B. P., Henderson, B. E., Frenkel, B., Haiman, C. A., Freedman, M., Tanay, A., and Coetzee, G. A. (2009) Functional enhancers at the gene-poor 8q24 cancer-linked locus. *PLoS Genet* **5**, e1000597
21. Kurdistani, S. K. (2012) Enhancer dysfunction: how the main regulators of gene expression contribute to cancer. *Genome biology* **13**, 156
22. Loven, J., Hoke, H. A., Lin, C. Y., Lau, A., Orlando, D. A., Vakoc, C. R., Bradner, J. E., Lee, T. I., and Young, R. A. (2013) Selective inhibition of tumor oncogenes by disruption of super-enhancers. *Cell* **153**, 320-334
23. Ryan, R. J., Drier, Y., Whitton, H., Cotton, M. J., Kaur, J., Issner, R., Gillespie, S., Epstein, C. B., Nardi, V., Sohani, A. R., Hochberg, E. P., and Bernstein, B. E. (2015) Detection of Enhancer-Associated Rearrangements Reveals Mechanisms of Oncogene Dysregulation in B-cell Lymphoma. *Cancer Discov* **5**, 1058-1071
24. Dawson, M. A., Kouzarides, T., and Huntly, B. J. (2012) Targeting epigenetic readers in cancer. *N Engl J Med* **367**, 647-657
25. Morgan, M. A., and Shilatifard, A. (2015) Chromatin signatures of cancer. *Genes Dev* **29**, 238-249
26. Kandoth, C., McLellan, M. D., Vandin, F., Ye, K., Niu, B., Lu, C., Xie, M., Zhang, Q., McMichael, J. F., Wyczalkowski, M. A., Leiserson, M. D. M., Miller, C. A., Welch, J. S., Walter, M. J., Wendl, M. C., Ley, T. J., Wilson, R. K., Raphael, B. J., and Ding, L. (2013) Mutational landscape and significance across 12 major cancer types. *Nature* **502**, 333-339
27. Lawrence, M. S., Stojanov, P., Mermel, C. H., Robinson, J. T., Garraway, L. A., Golub, T. R., Meyerson, M., Gabriel, S. B., Lander, E. S., and Getz, G. (2014) Discovery and saturation analysis of cancer genes across 21 tumour types. *Nature* **505**, 495-501
28. Herz, H. M., Hu, D., and Shilatifard, A. (2014) Enhancer malfunction in cancer. *Mol Cell* **53**, 859-866
29. Olivier, M., Hollstein, M., and Hainaut, P. (2010) TP53 mutations in human cancers: origins, consequences, and clinical use. *Cold Spring Harbor perspectives in biology* **2**, a001008
30. Brosh, R., and Rotter, V. (2009) When mutants gain new powers: news from the mutant p53 field. *Nat Rev Cancer* **9**, 701-713
31. Oren, M., and Rotter, V. (2010) Mutant p53 gain-of-function in cancer. *Cold Spring Harbor perspectives in biology* **2**, a001107
32. Sigal, A., and Rotter, V. (2000) Oncogenic mutations of the p53 tumor suppressor: the demons of the guardian of the genome. *Cancer Res* **60**, 6788-6793
33. Beckerman, R., and Prives, C. (2010) Transcriptional regulation by p53. *Cold Spring Harbor perspectives in biology* **2**, a000935
34. Freed-Pastor, W. A., and Prives, C. (2012) Mutant p53: one name, many proteins. *Genes Dev* **26**, 1268-1286
35. Di Agostino, S., Strano, S., Emiliozzi, V., Zerbini, V., Mottolese, M., Sacchi, A., Blandino, G., and Piaggio, G. (2006) Gain of function of mutant p53: the mutant p53/NF-Y protein complex reveals an aberrant transcriptional mechanism of cell cycle regulation. *Cancer cell* **10**, 191-202
36. Fontemaggi, G., Dell'Orso, S., Trisciuoglio, D., Shay, T., Melucci, E., Fazi, F., Terrenato, I., Mottolese, M., Muti, P., Domany, E., Del Bufalo, D., Strano, S., and Blandino, G. (2009) The execution of the transcriptional axis mutant p53, E2F1 and ID4 promotes tumor neo-angiogenesis. *Nat Struct Mol Biol* **16**, 1086-1093
37. Stambolsky, P., Tabach, Y., Fontemaggi, G., Weisz, L., Maor-Aloni, R., Siegfried, Z., Shiff, I., Kogan, I., Shay, M., Kalo, E., Blandino, G., Simon, I., Oren, M., and Rotter, V. (2010) Modulation of the vitamin D3 response by cancer-associated mutant p53. *Cancer cell* **17**, 273-285
38. Zhu, J., Sammons, M. A., Donahue, G., Dou, Z., Vedadi, M., Getlik, M., Barsyte-Lovejoy, D., Al-awar, R., Katona, B. W., Shilatifard, A., Huang, J., Hua, X., Arrowsmith, C. H., and Berger, S. L. (2015) Gain-of-function p53 mutants co-opt chromatin pathways to drive cancer growth. *Nature* **525**, 206-211
39. Rahnamoun, H., Lu, H., Duttke, S. H., Benner, C., Glass, C. K., and Lauberth, S. M. (2017) Mutant p53 shapes the enhancer landscape of cancer cells in response to chronic immune signaling. *Nat Commun* **8**, 754
40. Cho, Y. W., Hong, S., and Ge, K. (2012) Affinity purification of MLL3/MLL4 histone H3K4 methyltransferase complex. *Methods Mol Biol* **809**, 465-472

41. Lee, J., Kim, D. H., Lee, S., Yang, Q. H., Lee, D. K., Lee, S. K., Roeder, R. G., and Lee, J. W. (2009) A tumor suppressive coactivator complex of p53 containing ASC-2 and histone H3-lysine-4 methyltransferase MLL3 or its paralogue MLL4. *Proc Natl Acad Sci U S A* **106**, 8513-8518
42. Lauberth, S. M., Nakayama, T., Wu, X., Ferris, A. L., Tang, Z., Hughes, S. H., and Roeder, R. G. (2013) H3K4me3 interactions with TAF3 regulate preinitiation complex assembly and selective gene activation. *Cell* **152**, 1021-1036
43. Shinsky, S. A., and Cosgrove, M. S. (2015) Unique Role of the WD-40 Repeat Protein 5 (WDR5) Subunit within the Mixed Lineage Leukemia 3 (MLL3) Histone Methyltransferase Complex. *J Biol Chem* **290**, 25819-25833
44. Wang, S. P., Tang, Z., Chen, C. W., Shimada, M., Koche, R. P., Wang, L. H., Nakadai, T., Chramiec, A., Krivtsov, A. V., Armstrong, S. A., and Roeder, R. G. (2017) A UTX-MLL4-p300 Transcriptional Regulatory Network Coordinately Shapes Active Enhancer Landscapes for Eliciting Transcription. *Mol Cell* **67**, 308-321 e306
45. Chuikov, S., Kurash, J. K., Wilson, J. R., Xiao, B., Justin, N., Ivanov, G. S., McKinney, K., Tempst, P., Prives, C., Gamblin, S. J., Barlev, N. A., and Reinberg, D. (2004) Regulation of p53 activity through lysine methylation. *Nature* **432**, 353-360
46. Laptenko, O., Tong, D. R., Manfredi, J., and Prives, C. (2016) The Tail That Wags the Dog: How the Disordered C-Terminal Domain Controls the Transcriptional Activities of the p53 Tumor-Suppressor Protein. *Trends Biochem Sci* **41**, 1022-1034
47. Rao, R. C., and Dou, Y. (2015) Hijacked in cancer: the KMT2 (MLL) family of methyltransferases. *Nat Rev Cancer* **15**, 334-346
48. Dorighi, K. M., Swigut, T., Henriques, T., Bhanu, N. V., Scruggs, B. S., Nady, N., Still, C. D., 2nd, Garcia, B. A., Adelman, K., and Wysocka, J. (2017) Mll3 and Mll4 Facilitate Enhancer RNA Synthesis and Transcription from Promoters Independently of H3K4 Monomethylation. *Mol Cell* **66**, 568-576 e564
49. Jeong, K. W., Kim, K., Situ, A. J., Ulmer, T. S., An, W., and Stallcup, M. R. (2011) Recognition of enhancer element-specific histone methylation by TIP60 in transcriptional activation. *Nat Struct Mol Biol* **18**, 1358-1365
50. Yan, J., Chen, S. A., Local, A., Liu, T., Qiu, Y., Dorighi, K. M., Preissl, S., Rivera, C. M., Wang, C., Ye, Z., Ge, K., Hu, M., Wysocka, J., and Ren, B. (2018) Histone H3 lysine 4 monomethylation modulates long-range chromatin interactions at enhancers. *Cell Res* **28**, 204-220
51. Bereczki, O., Ujfaludi, Z., Pardi, N., Nagy, Z., Tora, L., Boros, I. M., and Balint, E. (2008) TATA binding protein associated factor 3 (TAF3) interacts with p53 and inhibits its function. *BMC Mol Biol* **9**, 57

Figure 1

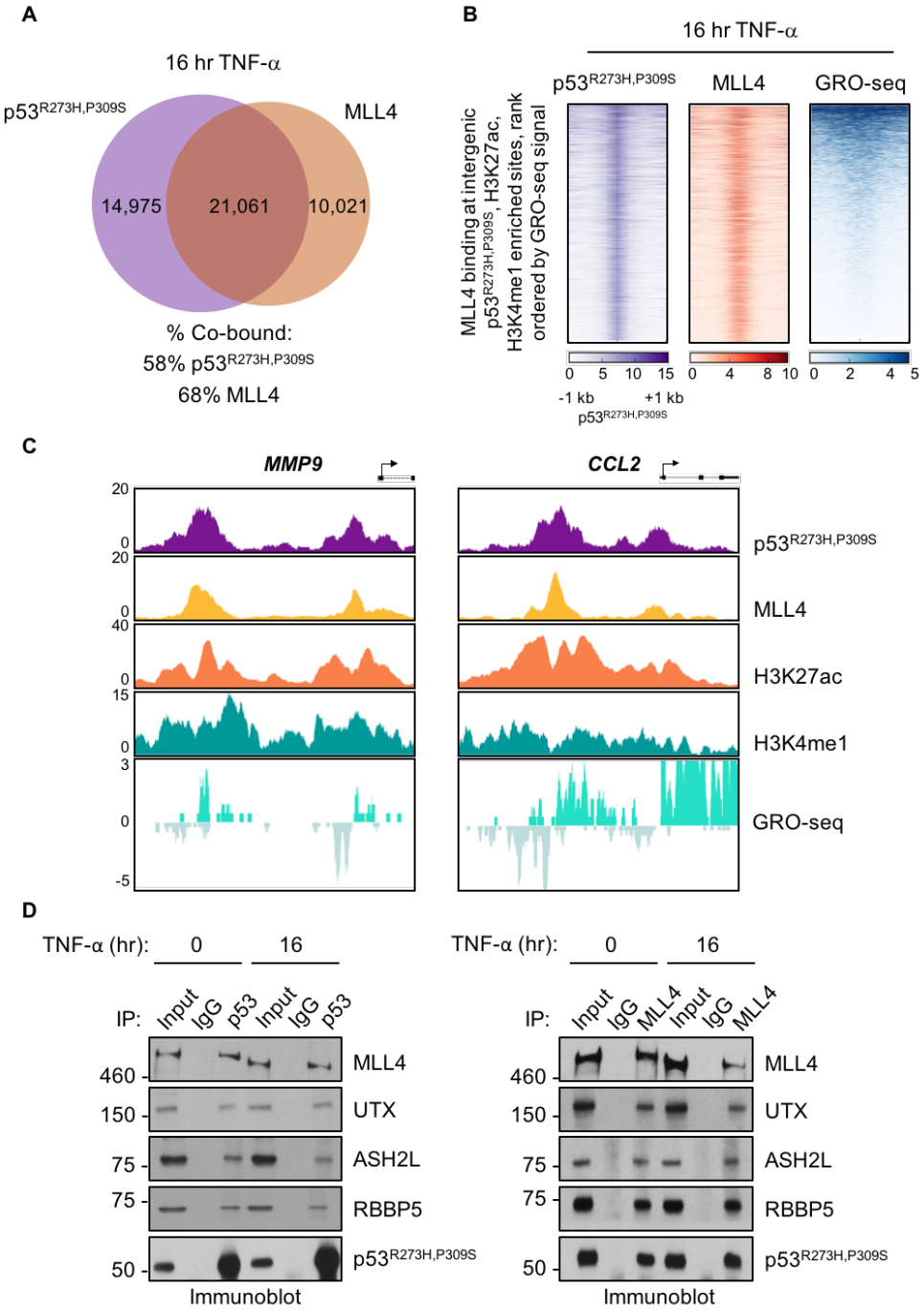

Figure 1. p53^{R273H,P309S} and MLL4 colocalize at active enhancers and form physiological associations in SW480 colon cancer cells.

A, Venn diagram depicting the overlapping ChIP-seq peaks for p53^{R273H,P309S} and MLL4 in SW480 cells following 16 hr TNF-α treatment. *B,* Heat maps of p53^{R273H,P309S} and MLL4 binding sites at intergenic regions enriched for p53^{R273H,P309S} and the histone marks, H3K4me1 and H3K27ac, and rank-ordered by GRO-seq signal in SW480 cells treated with TNF-α for 16 hr. Each row shows ± 1kb centered on p53^{R273H,P309S} peaks. *C,* UCSC genome browser images of p53^{R273H,P309S}, MLL4, H3K4me1, and H3K27ac ChIP-seq and GRO-seq signals at *MMP9* and *CCL2* gene loci. All ChIP-seq assays were performed as two biological replicates. *D,* Immunoblot analyses of p53^{R273H,P309S} (left) and MLL4 (right) co-immunoprecipitation (Co-IP) with lysates prepared from SW480 cells treated with TNF-α for 0 or 16 hr. All Co-IPs were performed three times, independently.

Figure 2

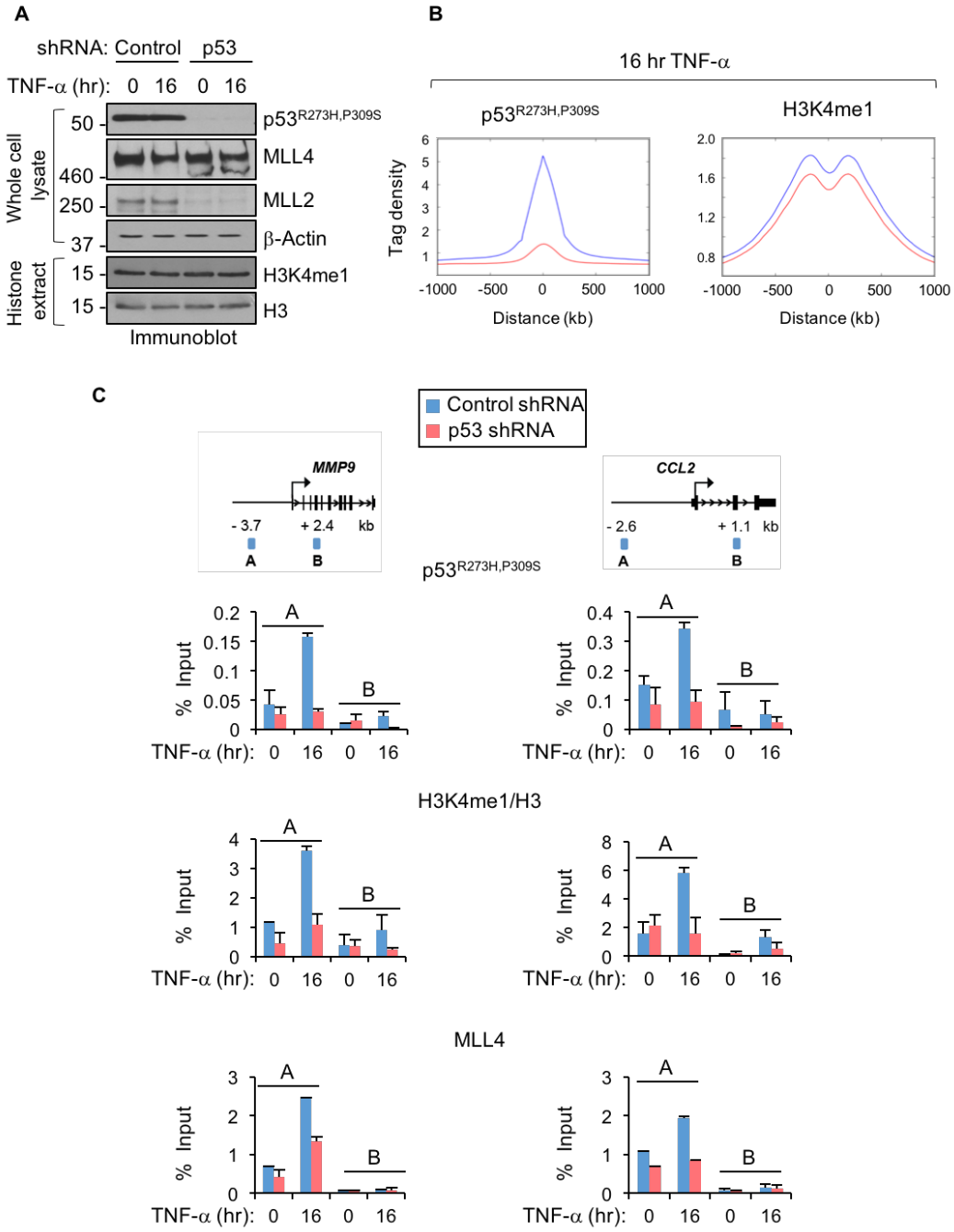

Figure 2. p53^{R273H,P309S} regulates H3K4me1 levels at enhancers in response to chronic immune signaling
A, Immunoblot analysis of whole cell lysates and histone extracts from SW480 cells stably expressing LacZ (control) or p53 (p53) shRNAs and treated with TNF-α for 0 or 16 hr with the indicated antibodies. *B*, The average signal intensity of p53^{R273H,P309S} and H3K4me1 ChIP-seq at intergenic regions in control and p53 knockdown cells treated with TNF-α for 16 hr. All ChIP-seq assays were performed as two biological replicates. *C*, ChIP-qPCR analyses of p53^{R273H,P309S} and MLL4 binding and H3K4me1 accumulation in SW480 cells treated as described in (A) at the enhancer (amplicon A) and nonspecific (amplicon B) regions of *MMP9* and *CCL2* gene loci. H3K4me1 enrichment levels were normalized to H3. Bar graphs represent the average of two independent ChIP experiments that are representative of at least three with error bars denoting the standard error.

Figure 3

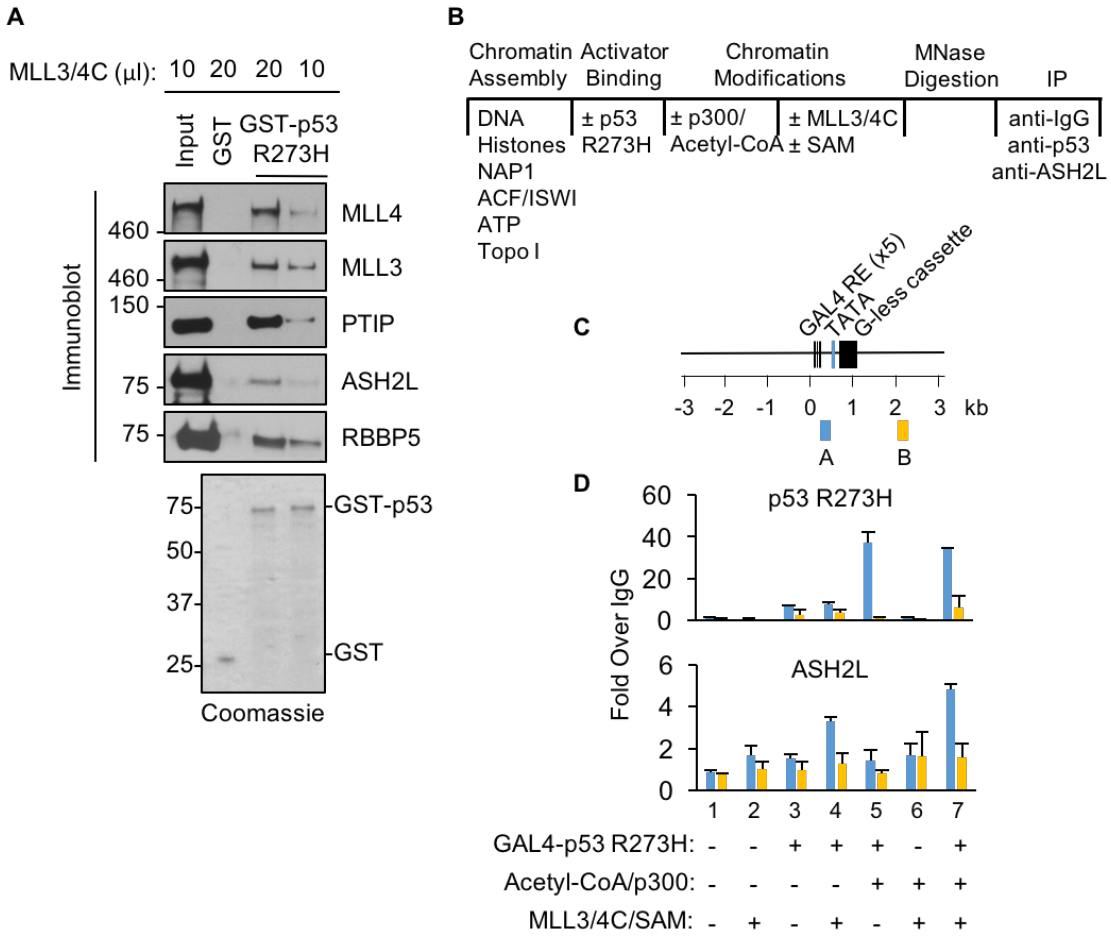

Figure 3. p53 R273H directly interacts with and regulates MLL3/4 binding to chromatin *in vitro*
A, (Top) Immunoblot analysis of the direct interaction between p53 R273H and MLL3/4C using (bottom) recombinant GST and GST-p53 R273H proteins analyzed by SDS-PAGE and Coomassie staining. Interaction assays were performed three times, independently. *B,* Schematic of the *in vitro* ChIP assay. *C,* Schematic of the pG_5ML template indicating the amplicons used for *in vitro* ChIP-qPCR. *D,* ChIP-qPCR analyses performed on recombinant chromatin templates using antibodies specific to p53 and ASH2L. Enrichment levels are calculated as fold enrichment over IgG. Bar graphs represent the average of two independent ChIP assays that are representative of at least three with error bars denoting the standard error.

Figure 4

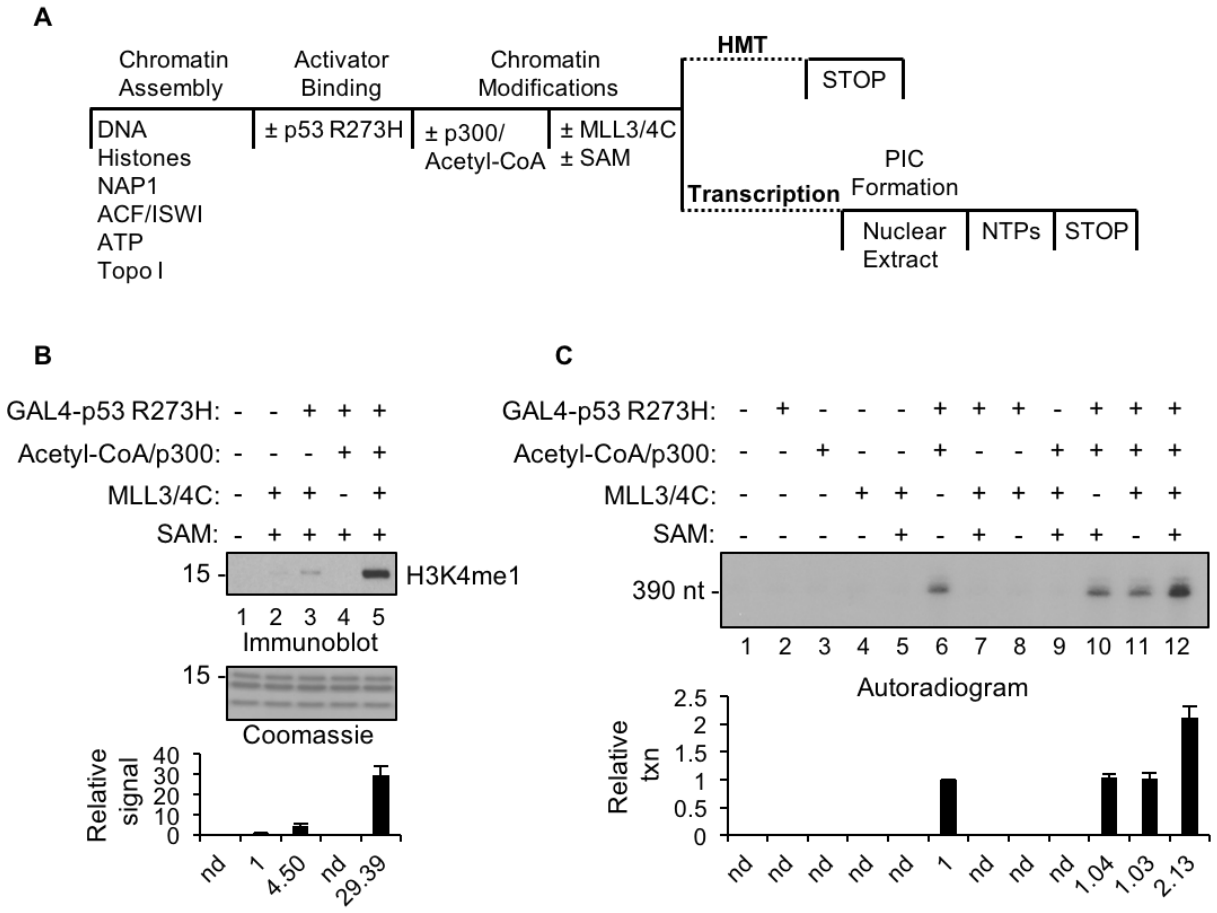

Figure 4. p53 R273H, MLL3/4C, and p300 cooperate to enhance the levels of histone methylation and transcriptional output, *in vitro*

A, Schematics of the *in vitro* HMT and transcription assays. *B,* (Top) Immunoblot analysis of H3K4me1 and (bottom) quantitation of the relative signal intensity of HMT assay performed with the indicated factors on chromatin templates. Quantitation analysis was performed using ImageJ with all values normalized to lane 2. Bar graphs represent the average of at least two independent experiments and error bars denote the standard error. Lower panel in (B) represents the loading of histones by SDS-PAGE and Coomassie staining. *C,* Nuclear extract-based transcription assay with indicated factors on chromatin templates. Relative transcription levels were quantitated using a phosphoimager. After background subtraction, all values were normalized to lane 6 with bar graphs representing the average of at least two independent experiments and error bars denoting the standard error. HMT and transcription assays were performed three times, independently.

Figure 5

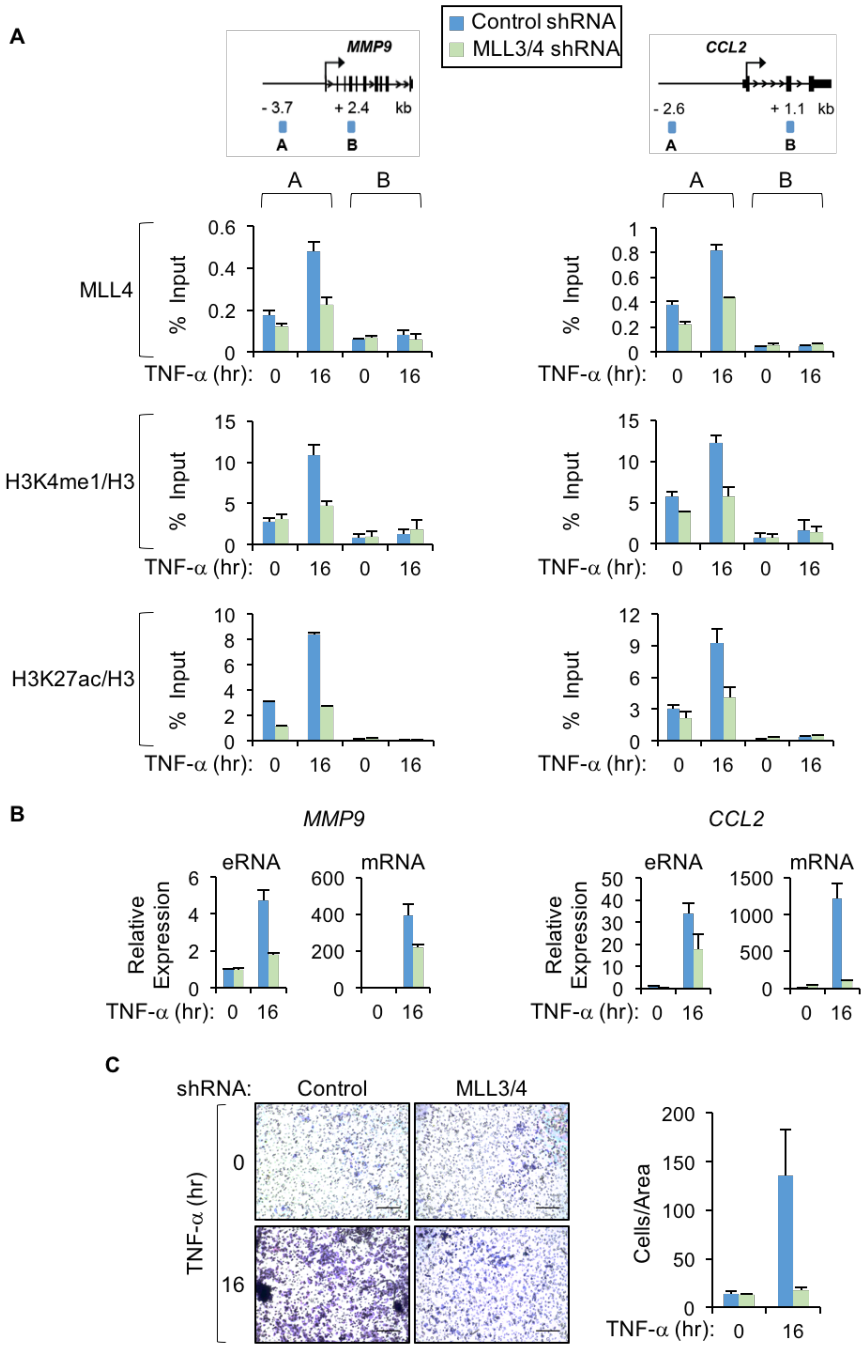

Figure 5. MLL3/4 regulates H3K4me1 deposition and enhancer activation that is linked to tumor promoting gene regulation and increased colon cancer cell invasion

A, ChIP-qPCR analyses of MLL4, H3K4me1, and H3K27ac at the enhancer (amplicon A) and nonspecific control (amplicon B) regions of *MMP9* and *CCL2* gene loci in SW480 cells stably expressing control (control) or MLL3 and MLL4 (MLL3/4) shRNAs and treated with TNF-α for 0 or 16 hr. ChIP-qPCR analysis of the histone marks, H3K4me1 and H3K27ac were normalized to H3. Bar graphs represent the average of two independent ChIP assays that are representative of at least three with error bars denoting the standard error. *B,* qRT-PCR analyses of *MMP9* and *CCL2* eRNAs and mRNAs in cells as described in (A). The expression levels shown after TNF-α are relative to the levels before treatment. Bar graphs represent the average of three independent experiments with error bars denoting the standard error. *C,* (Left) representative images and (right) quantitation of invasion assays performed with SW480 cells treated as described in (A) that were detected by Giemsa staining (scale bar: 0.2 mm). The bar graphs represent the average number of cells that invaded through the Matrigel-coated membrane from three independent experiments with error bars denoting the standard error.

Figure 6

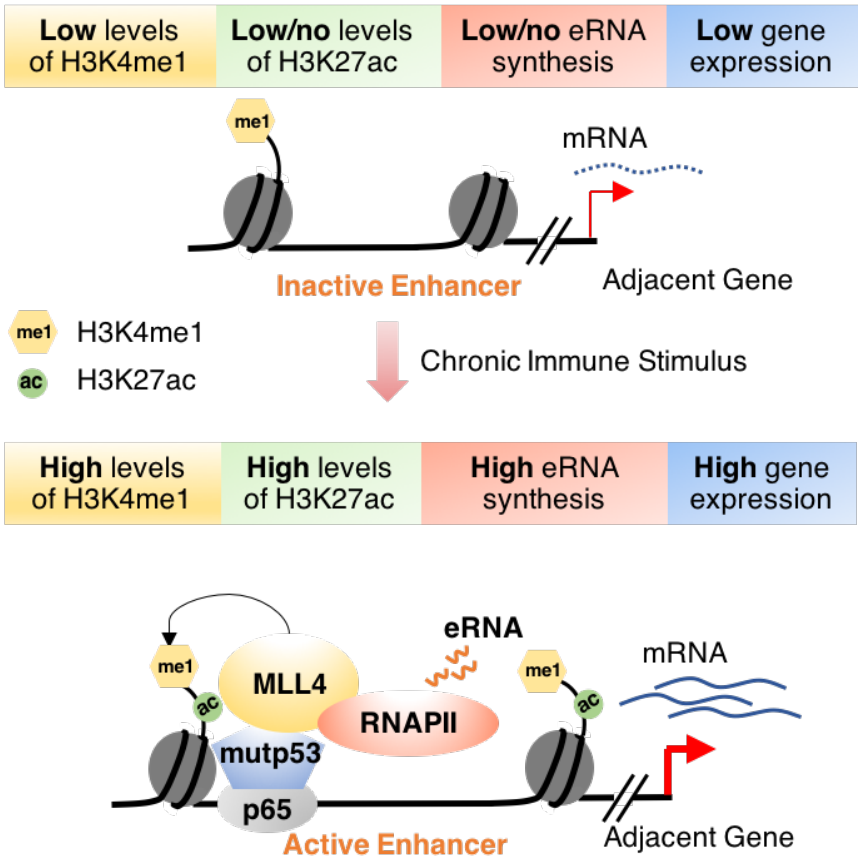

Figure 6. Proposed model for enhancer activation mediated by mutp53-MLL4 interactions
We propose a model in which mutp53 interactions with MLL4 results in alterations in H3K4me1 levels, enhancer activation, and the potent induction of tumor promoting gene expression in response to chronic TNF-α signaling. The contributions of NFκB/p65 were not examined in this study but was included in our model since NFκB/p65 contributes to mutp53 recruitment at these enhancers(39).

Mutant p53 regulates enhancer-associated H3K4 monomethylation through interactions with the methyltransferase MLL4

Homa Rahnamoun, Juyeong Hong, Zhengxi Sun, Jihoon Lee, Hanbin Lu and Shannon M Lauberth

J. Biol. Chem. published online June 28, 2018
